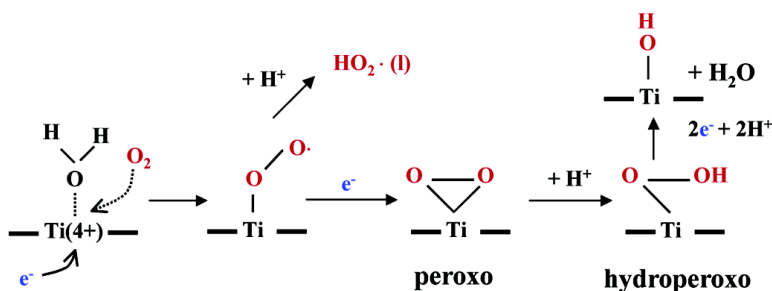Article

In Situ FTIR Studies of Primary Intermediates of Photocatalytic Reactions on Nanocrystalline TiO Films in Contact with Aqueous Solutions

Ryuhei Nakamura, Akihito Imanishi, Kei Murakoshi, and Yoshihiro Nakato

More About This Article

Additional resources and features associated with this article are available within the HTML version:

- Supporting Information
- Links to the 16 articles that cite this article, as of the time of this article download
- Access to high resolution figures
- Links to articles and content related to this article
- Copyright permission to reproduce figures and/or text from this article

View the Full Text HTML

In Situ FTIR Studies of Primary Intermediates of Photocatalytic Reactions on Nanocrystalline TiO$_2$ Films in Contact with Aqueous Solutions

Ryuhei Nakamura, Akihito Imanishi, Kei Murakoshi, and Yoshihiro Nakato*

Contribution from the Department of Chemistry, Graduate School of Engineering Science, Osaka University, Toyonaka, Osaka 560-8531, Japan

Received November 27, 2002; E-mail: nakato@chem.es.osaka-u.ac.jp

Abstract: Multiple internal reflection infrared spectroscopy was applied to in situ investigations of surface intermediates of photocatalytic reactions on nanocrystalline TiO$_2$ films in contact with aqueous solutions. UV irradiation in the presence of dissolved O$_2$ caused the appearance of new bands peaked at 943, 838, and 1250–1120 cm^{-1} together with intensity changes in other bands. Investigations of influences of the solution pH, the presence or absence of hole and electron scavengers, and isotopic H$_2$O → D$_2$O exchange on the spectral changes have revealed that the primary step of photocatalytic O$_2$ reduction is the formation of the surface peroxo species, Ti(O$_2$), giving the 943 cm^{-1} band, probably with the surface superoxo species, TiOO·, as a precursor, in neutral and acidic solutions. The surface peroxo species is then transformed to the surface hydroperoxo, TiOOH, giving the 838 and 1250–1120 cm^{-1} bands, by protonation in the dark. This is, to our knowledge, the first direct in situ spectroscopic detection of primary intermediates for the photocatalytic O$_2$ reduction in aqueous solutions. On the basis of the assignment, a possible reaction scheme for various processes of the photocatalytic O$_2$ reduction is proposed, which is in harmony with other spectral changes induced by the UV irradiation.

Introduction

Photocatalytic reactions on TiO$_2$ particles or thin films have been attracting much attention in view of their possible application to solar energy conversion (water splitting)[1,2] as well as photodecomposition of waste materials and harmful organic compounds.[3,4] Intensive work has been done on the reaction products, yields, and mechanisms,[5–8] to increase the reaction efficiencies and selectivity, but the details of the reaction mechanisms still remain unclear, most probably because of a shortage of in situ direct detection of active reaction intermediates by spectroscopic methods.

ESR spectroscopy is a useful method to investigate intermediate radicals, such as O$_2^-$, O$^-$, O$_3^-$, etc., formed on illuminated TiO$_2$ powder in air.[9–15] The method has a merit in that it can

be easily applied to aqueous systems. Jaeger and Bard[16] reported long ago, using a spin-trapping method, that hydroxyl (·OH) and perhydroxyl (HO$_2$·) radicals were produced on illuminated TiO$_2$ powder in aqueous solutions. Recently, Kaise et al.[17,18] used a flow-type ESR method to detect reaction intermediates more directly and reported that methyl (CH$_3$·) and carboxymethyl (·CH$_2$COOH) radicals were formed by photocatalytic decomposition of acetic acid on TiO$_2$ in aqueous solutions.

Infrared (IR) spectroscopy is another powerful method to study adsorbed species on solid surfaces.[19,20] This method can give fruitful information on the molecular structure, molecular orientation, and adsorption strength of surface species. Szczepankiewicz et al.[21,22] used diffuse reflectance IR Fourier transform spectroscopy (DRIFTS) and reported a new band at 3716 cm^{-1} for UV-irradiated TiO$_2$ powder in the gas phase in the presence of a hole scavenger. The band was assigned to

(1) Fujishima, A.; Honda, K. *Nature* **1972**, *238*, 37.
(2) Khan, S. U. M.; Al-Shahry, M.; Ingler, W. B., Jr. *Science* **2002**, *297*, 2243.
(3) Wang, R.; Hashimoto, K.; Chikuni, M.; Kojima, E.; Kitamura, A.; Shimohigashi, M.; Watanabe, T. *Nature* **1997**, *388*, 431.
(4) Asahi, R.; Morikawa, T.; Ohwaki, T.; Aoki, K.; Taga, Y. *Science* **2001**, *293*, 269.
(5) Ollis, D. S.; Al-Ekabi, H., Eds. *Photocatalytic Purification and Treatment of Water and Air*; Elsevier: Amsterdam, 1993.
(6) Fujishima, A.; Rao, T. N.; Tryk, D. A. *J. Photochem. Photobiol., C: Photochem. Rev.* **2000**, *1*, 1.
(7) Schiavello, M. *Heterogeneous Photocatalysis*; John Wiley & Sons Ltd.: New York, 1997.
(8) Hoffmann, M. R.; Martin, S. T.; Choi, W.; Bahnemann, D. W. *Chem. Rev.* **1995**, *95*, 69.
(9) Naccache, C.; Mariaudeau, P.; Che, M.; Tench, A. J. *Trans. Faraday. Soc.* **1971**, *67*, 506.
(10) Mariaudeau, P.; Vedrine, J. C. *J. Chem. Soc., Faraday Trans. 2* **1976**, *72*, 472.
(11) Gonzalez-Elipe, A. R.; Munuera, G.; Soria, J. *J. Chem. Soc., Faraday Trans.* **1979**, *75*, 748.
(12) How, R. F.; Grätzel, M. *J. Phys. Chem.* **1987**, *91*, 3906.

(13) Anpo, M.; Aikawa, N.; Kodama, S.; Kubokawa, Y. *J. Phys. Chem.* **1984**, *88*, 3998.
(14) Anpo, M.; Yabuta; Kodama, S.; Kubokawa, Y. *Bull. Chem. Soc. Jpn.* **1986**, *59*, 259.
(15) Einaga, H.; Ogata, A.; Futamura, S.; Ibusuki, T. *Chem. Phys. Lett.* **2001**, *338*, 303.
(16) Jaeger, C. D.; Bard, A. J. *J. Phys. Chem.* **1979**, *83*, 3146.
(17) Kaise, M.; Kondoh, H.; Nishihara, C.; Nozoe, H.; Shindo, H.; Nimura, S.; Kikuchi, O. *J. Chem. Soc., Chem. Commun.* **1993**, 395.
(18) Kaise, M.; Nagai, H.; Tokuhashi, K.; Kondo, S.; Nimura, S.; Kikuchi, O. *Langmuir* **1994**, *10*, 1345.
(19) Somorjai, G. A. *Introduction to Surface Chemistry and Catalysis*; John Wiley & Sons: New York, 1994; pp 324–329.
(20) Clark, R. J. H.; Hester, R. E. *Spectroscopy for Surface*; John Wiley & Sons: New York, 1998; pp 219–272.
(21) Szczepankiewicz, S. H.; Colussi, A. J.; Hoffmann, M. R. *J. Phys. Chem. B* **2000**, *104*, 9842.
(22) Szczepankiewicz, S. H.; Moss, J. A.; Hoffmann, M. R. *J. Phys. Chem. B* **2002**, *106*, 7654.

OH stretching for surface Ti(3+)OH formed by electron capture at acidic Ti(4+)OH centers. They also reported another band at 3683 cm^{-1} in an oxygen atmosphere in the absence of hole scavengers and ascribed it to a surface-bound OH· radical formed by hole capture at Ti(4+)OH centers. Recently, Sato et al.[23−25] applied surface-enhanced IR absorption spectroscopy (SEIRAS) to the investigation of gas-phase photocatalytic reactions on platinized TiO$_2$. They succeeded in direct observation of methyl radical (CH$_3$·) formed by photodecomposition of acetic acid and reported that the formation rate was significantly enhanced by Pt deposition.[23]

It is well known that the IR spectroscopy has a serious difficulty in application to aqueous systems because of the strong IR absorption of water.[19,20] The difficulty can be overcome to a large extent by using internal reflection techniques, in which evanescent IR waves penetrate only into a thin layer of an aqueous solution to the thickness of about a few micrometers from the surface of the internal reflection element (IRE), so that the IR absorption of water can be minimized.[26] A large amount of work has thus been done on the internal reflection techniques of both single- and multireflection modes as well as their application to in situ studies of adsorbed species on thin films, as reviewed in a recent book.[27] Very recently, McQuillan et al. applied the single internal reflection (SIR) technique with a ZnSe prism as the IRE to studies of ionic surfactants,[28] aromatic carboxylic acids,[29] phosphates,[30,31] bacteria,[32] and ruthenium(II) complexes[33] adsorbed on various metal oxides such as TiO$_2$, ZrO$_2$, Al$_2$O$_3$, and Ta$_2$O$_5$ in aqueous media. Osawa applied a similar technique to electrochemical systems,[35] and Baiker et al. applied one to heterogeneous catalytic systems.[36,37] The application of the internal reflection techniques to photocatalytic systems is, however, quite limited. Only McQuillan et al. reported,[38] using the single internal reflection technique with the ZnSe IRE, that glyoxylic acid adsorbed on particulate TiO$_2$ in aqueous solutions was transformed to oxalate by UV irradiation.

In the present work, we have applied the highly sensitive multiple internal reflection (MIR) technique to in situ studies of photocatalytic processes on the TiO$_2$ surface in contact with aqueous solutions. The focus was placed on the O$_2$ reduction by photoexcited electrons, because active oxygen species produced by this reaction are known to be crucially important for photocatalytic oxidation of organic compounds.[39,40] We have succeeded in detecting primary intermediates of the photocata-
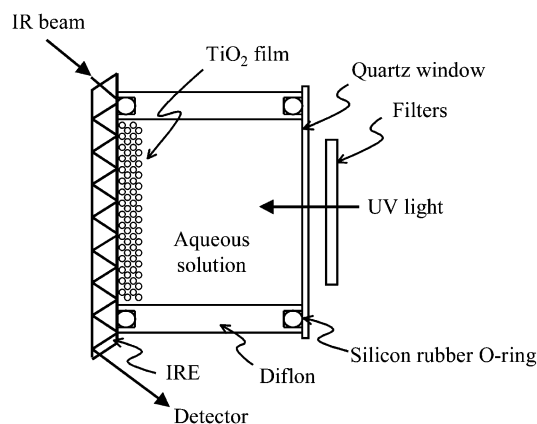

Figure 1. Schematic illustration of a spectral cell used for in situ MIR-IR measurements.

lytic O$_2$ reduction that have been only assumed for a long time by many workers, spectroscopically under in situ conditions.

Experimental Section

Two types of nanocrystalline TiO$_2$ particles, JRC-TIO-2 and JRC-TIO-5, were obtained from the Catalysis Society of Japan. The samples were well characterized in the Society as the reference catalysts. JRC-TIO-2 is composed of 100% anatase with an average primary particle diameter (d_{av}) of 80 nm and a surface area of 16 m^2/g. JRC-TIO-5 is composed of 90.7% rutile and 9.3% anatase with d_{av} = 640 nm and a surface area of 3 m^2/g. Before experiments, the surfaces of TiO$_2$ particles were cleaned by heating at 500 °C in an O$_2$ atmosphere for 5 h and UV irradiation in O$_2$-saturated water for 1 h, followed by sonication for 30 min. The cleaned TiO$_2$ particles were, after drying, kept under vacuum (<1 × 10^{-3} Torr). All chemicals, D$_2$O (Aldrich, 99.9 at. %), NaOH (Wako), HCl (Wako), NaOD (Aldrich, 99.9 at. %), ethanol (Wako), and FeCl$_3$ (Aldrich), were of reagent grade and used as received. All solutions were prepared using pure (Milli-Q) water with a conductivity of 18 MΩ^{-1} cm^{-1}.

The spectral cell for multiple internal reflection infrared (MIRIR) experiments is shown schematically in Figure 1. A trapezoidal-shaped ZnSe internal reflection element (IRE) (50 mm × 20 mm × 2 mm, 45° incident angle) was obtained from Pier Optics Co., Ltd., Japan. A particulate TiO$_2$ film was applied on one face of the IRE by a dip-coating method. The IRE was dipped in a 0.01 M TiO$_2$ aqueous suspension and dried in air, followed by wiping of the rear face of the IRE with a soft cloth. This procedure was repeated five times. The TiO$_2$-coated IRE thus obtained was set in the spectral cell made by Diflon (Figure 1). The inner volume of the cell was approximately 10 mL. The length and width of the exposed area of the IRE are 35.5 and 9.2 mm, respectively. The IR light was reflected about 9 times in the IRE with TiO$_2$, as calculated from the geometry of the IRE. The structure of the TiO$_2$ films was inspected with a Hitachi S-5000 scanning electron microscope (SEM).

The spectral cell was placed in the sample chamber of an FTIR spectrometer (Bio-Rad FTS 575C) with a deuterated triglycine sulfate (DTGS) detector. Before measurements, the sample chamber was purged with dry air, and the TiO$_2$ film was kept in the dark for about 60 min. The IR intensity (I) versus wavelength (λ) was obtained by averaging 100 scans at a resolution of 4 cm^{-1}, with a processing time of 1.5 min for one spectrum. All MIRIR absorption spectra were obtained in the form of absorbance, log(I_0/I), using an appropriate reference sample giving I_0. The frequency range in the present work was from 4000 to 650 cm^{-1}. The increase in the thickness and length of the TiO$_2$ film on the IRE reduced the total output IR intensity from the IRE in a region below 1000 cm^{-1} where TiO$_2$ absorbs light, making the spectrum noisy, whereas the decrease in the thickness and length weakened the signals (UV irradiation-induced spectral changes)

(23) Sato, S.; Ueda, K.; Kawasaki, K.; Nakamura, R. *J. Phys. Chem. B* **2002**, *106*, 9054.
(24) Nakamura, R.; Sato, S. *Langmuir* **2002**, *18*, 4433.
(25) Nakamura, R.; Sato, S. *Langmuir* **2001**, *17*, 2298.
(26) Harrick, N. J. *Internal Reflection Spectroscopy*; John Wiley & Sons: New York, 1967.
(27) Suëtaka. W. *Surface Infrared and Raman Spectroscopy*; Plenum Press: New York, 1996.
(28) Dobson, K. D.; Roddick-Lanzilotta, A. D.; McQuillan, A. J. *Vib. Spectrosc.* **2000**, *24*, 287.
(29) Dobson, K. D.; McQuillan, A. J. *Spectrochim. Acta, Part A* **2000**, *56*, 557.
(30) Connor, P. A.; McQuillan, A. J. *Langmuir* **1999**, *15*, 2916.
(31) Ronson, T. K.; McQuillan, A. J. *Langmuir* **2002**, *18*, 5019.
(32) McWhirter, M. J.; McQuillan, A. J.; Bremer, P. J. *Colloids Surf., B* **2002**, *26*, 365.
(33) Nazeeruddin, M. K.; Amirnasr, M.; Comte, P.; Mackay, J. R.; McQuillan, A. J.; Houriet, R.; Grätzel, M. *Langmuir* **2000**, *16*, 8525.
(34) Connor, P. A.; Dobson, K. D.; McQuillan, A. J. *Langmuir* **1999**, *15*, 2402.
(35) Osawa, M. *Bull. Chem. Soc. Jpn.* **1997**, *70*, 2861.
(36) Ferri, D.; Buergi, T.; Baiker, A. *J. Phys. Chem. B* **2001**, *105*, 3187.
(37) Buürgi, T.; Baiker, A. *J. Phys. Chem. B* **2002**, *106*, 10649.
(38) Ekström, G. N.; McQuillan, A. J. *J. Phys. Chem. B* **1999**, *103*, 10562.
(39) Gerischer, H.; Heller, A. *J. Electrochem. Soc.* **1992**, *139*, 113.
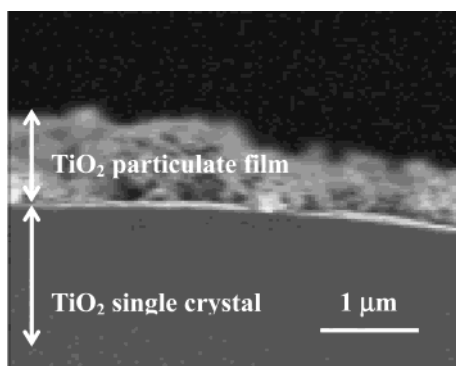(40) Nakamura, R.; Sato, S. *J. Phys. Chem. B* **2002**, *106*, 5893.

Figure 2. Cross-sectional SEM of a TiO₂ particulate film on a single-crystal TiO₂ wafer.

themselves. The S/N ratio of more than 10 was obtained even at 750 cm^{-1} in the present work, by optimizing the thickness and length of the TiO₂ film.

UV illumination of the TiO₂ film in the spectral cell was performed using a 200 W Hg−Xe lamp (Hypercure 200 UV, Yamashita Denso) equipped with an optical guide. The light in wavelengths from 240 to 400 nm was chosen with a band-pass filter (Toshiba UV-D33S). A neutral density (metal net) filter and an IR-cut filter were also used to avoid cell heating. The incident UV light intensity at the position of the sample surface was approximately 20 mW cm^{-2}, as measured with a thermopile (Eppley Laboratory).

ZnSe used as the IRE is a semiconductor with a band gap of 2.7 eV and is not stable in strongly acidic and alkaline solutions. Therefore, much care was taken to prevent the occurrence of dark and photo-induced reactions at the ZnSe surface that will affect the IR spectra. We confirmed that UV irradiation of ZnSe with TiO₂ films for 30 min in aqueous solutions caused no coloring nor etching (pitting) at the ZnSe surface. Also, UV irradiation of ZnSe without TiO₂ for 30 min in aqueous solutions caused no change in the MIRIR spectrum, except a slight broad decline below 1000 cm^{-1}. Essentially the same results were obtained between the ZnSe-IRE and an IRE of germanium (Ge) with a much smaller band gap of about 0.7 eV.

Results

Figure 2 shows a cross-sectional SEM of a TiO₂ (TIO-2, anatase) film, prepared on a TiO₂ single-crystal wafer by the dip-coating method. The thickness of the film is about 1 μm, which is of the same order in magnitude as the length of penetration of evanescent IR waves from the ZnSe IRE into an aqueous solution.[41] The UV irradiation for the photocatalytic reaction was carried out from the side of the TiO₂/solution interface (Figure 1). The penetration depth (α^{-1}) of the UV light is of the order of several hundred nanometers ($\alpha^{-1} = 250$ nm at $\lambda = 380$ nm),[42,43] which is also of the same order in magnitude as the TiO₂ film thickness.

Figure 3A shows an MIRIR spectrum of a particulate TiO₂ film (TIO-5, mainly rutile) in contact with pure water before UV irradiation. A ZnSe prism with no TiO₂ was used as the reference sample. A broad band peaked at 3350 cm^{-1} and a relatively sharp band at 1647 cm^{-1} can be assigned to the OH stretching and the HOH bending modes of water, respectively. Weak bands in a region from 2990 to 2850 cm^{-1} can be assigned to the CH stretching of hydrocarbon contamination at the TiO₂
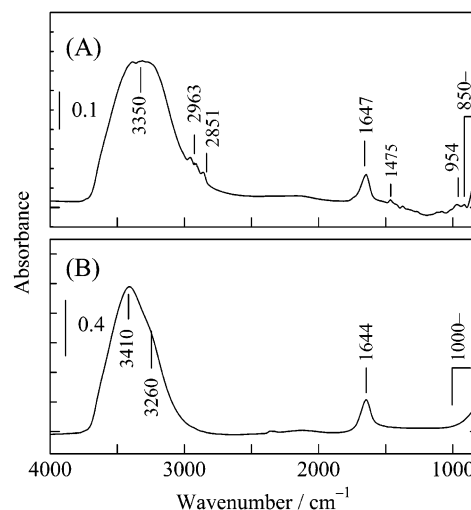

Figure 3. (A) A MIR-IR spectrum of a TiO₂ (TIO-5, mainly rutile) film in contact with pure water, and (B) a transmission FTIR spectrum of bulk water.

surface, which could not be removed by a heat treatment at 500 °C in O₂, as discussed later. A weak band at 1475 cm^{-1} may be assigned to carbonate (CO_3^{2-}) ions[44] at the TiO₂ surface. Relatively strong absorption observed below 850 cm^{-1} is due to lattice vibrations of TiO₂.[45] The origin of a weak band at 954 cm^{-1} is not clear; it might be assigned to the antisymmetric Ti−O stretching mode of the Ti−O−Ti[34,46] at the TiO₂ surface. For comparison, Figure 3B shows a transmission FTIR spectrum of pure water. The OH stretching and HOH bending modes appear at 3410 and 1644 cm^{-1}, respectively. The shoulder at about 3260 cm^{-1} is assigned to the Fermi resonance between the OH stretching and the binary overtone of the HOH bending modes.[47] A slight swelling from 2000 to 2300 cm^{-1} can be ascribed to the second overtone of the vibrational mode of water.[48] It should be noted that the OH stretching and HOH bending modes in spectrum A are slightly different in both spectral position and shape from those in spectrum B. Besides, the vibrational mode of water[48] below 1000 cm^{-1} appearing in spectrum B is not observed in spectrum A. These results suggest that spectrum A really detects water within the TiO₂ film, which is in a slightly different situation from bulk water, as reported by McQuillan et al.[34]

Figure 4A shows the MIRIR spectra of a TiO₂ (TIO-5) film in contact with O₂-saturated pure water as a function of the UV-irradiation time. The spectrum of the TiO₂ film before UV irradiation was taken as the spectral reference. A significant decrease in the band intensity at 3377 cm^{-1} in spectrum c suggests that the amount of water within the TiO₂ film decreased by the irradiation. The origin of weak bands at 3693 and 3645 cm^{-1} is not clear at present. McQuillan et al. reported similar bands at 3600 and 3480 cm^{-1} and interpreted them as indicating the formation of hydroxyls weakly bound to the surface or interfacial water which is free from a hydrogen bond with bulk water.[34] The appearance of broad bands in regions of 1250−1120 and 1100−870 cm^{-1} indicates the formation of some new

(41) The intensity of the evanescent wave reaches 1/e at 0.9 μm from the ZnSe surface with a wavenumber of 1650 cm^{-1}.
(42) Eagles, D. M. *J. Phys. Chem. Solids* **1964**, *25*, 1243.
(43) Poznyak, K. S.; Sviridov, V. V.; Kulak, A. I.; Samtsov, M. P. *J. Electroanal. Chem.* **1992**, *340*, 73.
(44) Yates, D. J. C. *J. Phys. Chem.* **1961**, *65*, 746.
(45) Farmer, V. C., Ed. *The Infrared Spectra of Minerals*; Mineral Society: London, 1974.
(46) Kushto, G. P.; Zhou, M.; Andrews, L.; Bauschlicher, C. W. *J. Phys. Chem. A* **1999**, *103*, 1115.
(47) Ataka, K.; Yotsuyanagi, T.; Osawa, M. *J. Phys. Chem.* **1996**, *100*, 10664.
(48) Devlin, J. P.; Sadlej, J.; Buch, V. *J. Phys. Chem. A* **2001**, *105*, 974.
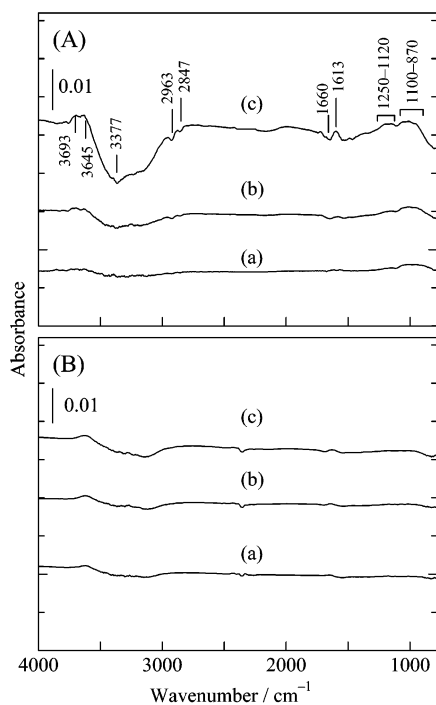
Figure 4. MIR-IR spectra of a TiO_2 (TIO-5) film in (A) O_2- and (B) N_2-saturated pure water as a function of the UV-irradiation time: (a) 8 min, (b) 16 min, and (c) 24 min. The TiO_2 film before the UV irradiation is used as the reference sample.

species, as discussed later. Decreases in the band intensity at 2963 and 2847 cm^{-1} can be attributed to removal of the aforementioned contaminating hydrocarbons at the TiO_2 surface by photoinduced oxidation reactions. A swelling at 1613 cm^{-1} and a depression at 1660 cm^{-1} might tentatively be attributed to a slight lower-energy shift of the bending mode of water at 1647 cm^{-1}. Similar but less marked changes in spectra were observed for TiO_2 films in contact with N_2-bubbled (deoxygenated) pure water, as shown in Figure 4B, indicating that the spectral changes of Figure 4A are caused by photocatalytic reduction of dissolved oxygen.

Figure 5 shows time courses of the MIRIR spectra in the region from 1550 to 750 cm^{-1} in an expanded form. The spectral changes by UV irradiation for TiO_2 (TIO-5) films in contact with O_2-saturated aqueous solutions strongly depended on the solution pH. For a neutral solution of pH 7 (Figure 5B), two bands appeared at 1023 and 943 cm^{-1}, together with a broad band in the 1250−1120 cm^{-1} region. The spectral change in an acidic solution of pH 4.5 (Figure 5A) was rather similar to that in the neutral solution, except that the band at 1023 cm^{-1} became weaker, whereas the 1250−1120 cm^{-1} band became stronger. In addition, new bands appeared at around 887 and 838 cm^{-1}. The spectral change in an alkaline solution of pH 11.8 (Figure 5C) is, on the other hand, considerably different from those for the neutral and acidic solutions, showing the appearance of only the sharp band at 943 cm^{-1}. An extended tail on the higher-energy side will most probably be attributed to slight overlapping of other bands, because the tail is essentially removed in isotope-effect experiments, as explained later (Figure 10B). From these results, it is apparent that at least two individual species are photoproduced at the TiO_2 surface, one giving the 943 cm^{-1} band and the other giving the 1250−1120 cm^{-1} band, which will hereafter be referred to as species X and Y, respectively.
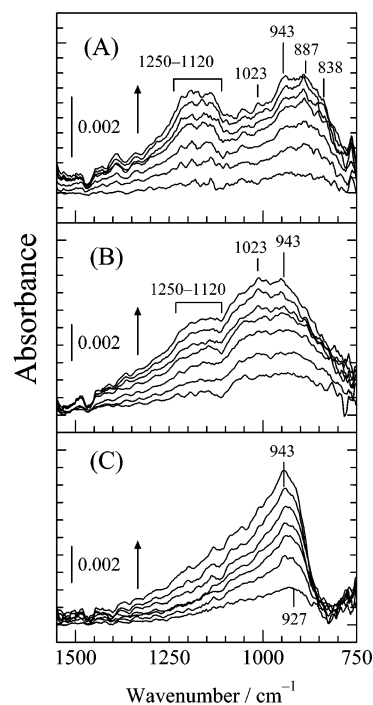

Figure 5. Time courses of MIR-IR spectra for TiO_2 (TIO-5) films in O_2-saturated aqueous solutions of pH (a) 4.5, (b) 7.0, and (c) 11.8. Spectra were recorded in times of 3, 6, 9, 12, 15, 18, and 21 min after the start of UV irradiation. The absorbance was changed nearly parallel to the irradiation time. Arrows in the figure indicate the direction of spectral changes with time.
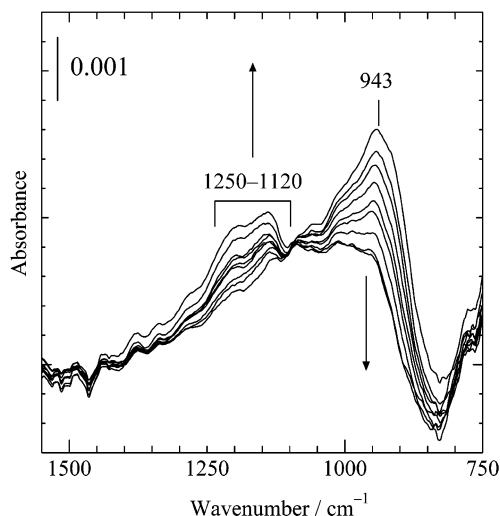

Figure 6. Time course of the MIR-IR spectrum for a TiO_2 film (TIO-5) in an O_2-saturated alkaline solution of pH 11.8 in the dark after the stop of UV irradiation for 21 min. Spectra were recorded in 0, 6, 9, 15, 21, 24, 30, 60, and 80 min after the stop of the UV irradiation. Arrows in the figure indicate the direction of spectral changes with time.

To clarify the chemical origins for species X and Y, we measured the time courses of the MIRIR spectra in the dark after stopping the UV irradiation. The 943 cm^{-1} band for the alkaline solution (Figure 5C) became weaker, whereas the 1250−1120 cm^{-1} band became stronger, as shown in Figure 6, suggesting that species X was transformed into species Y. Figure 7 compares the changes of the peak intensities for the 943 and 1250−1120 cm^{-1} bands between pH 4.5 and 11.8 in the dark after stopping the UV irradiation. In both solutions, the amount of X decreases and that of Y increases, but the rate of the change
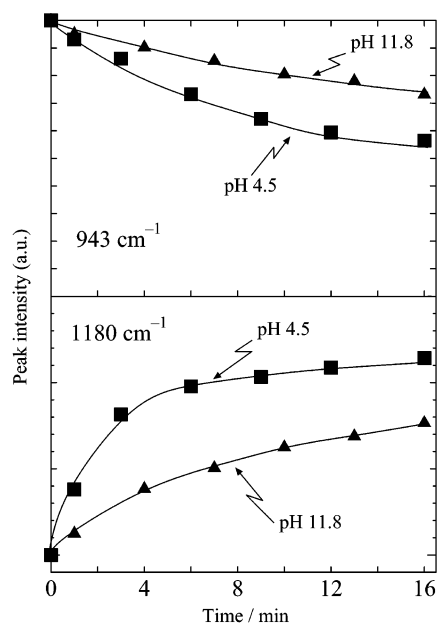
Figure 7. The band intensities at 943 and 1180 cm^{-1} in O$_2$-saturated aqueous solutions of pH 11.8 and 4.5 as a function of time in the dark after the stop of UV irradiation.
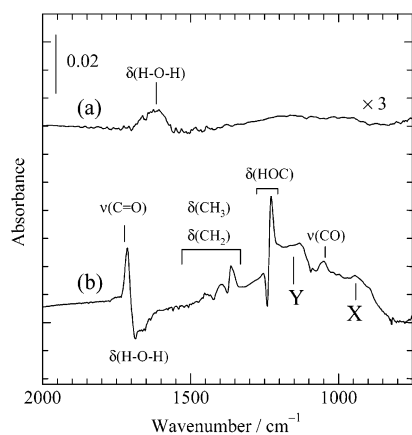

Figure 8. MIR-IR spectra for a TiO$_2$ (TIO-5) film after 21-min UV irradiation in O$_2$-saturated aqueous solutions containing (a) 10 mM Fe^{3+} and (b) 25 wt % ethanol.

is higher in the acidic solution than that in the alkaline solution. This result strongly suggests that the transformation of X to Y is caused by protonation.

We mentioned earlier that the spectral changes were caused by the photocatalytic reduction of dissolved O$_2$. To confirm the conclusion, we examined the effect of addition of Fe^{3+} and ethanol to the aqueous solution, because Fe^{3+} and ethanol are known to act as efficient electron and hole scavengers, respectively. The UV irradiation in the presence of Fe^{3+} gave no absorption bands at 943 and 1250−1120 cm^{-1}, assigned to species X and Y (Figure 8a), whereas that in the presence of ethanol gave these bands (Figure 8b), although the spectrum was made complex by mixing of absorption bands assigned to ν(C=O), δ(CH$_3$), δ(CH$_2$), δ(HOC), and ν(CO) of acetaldehyde formed by photooxidation of ethanol. Figure 9 shows the peak intensity at 943 cm^{-1} versus time in the presence of Fe^{3+} and ethanol. The addition of ethanol enhanced the appearance of the 943 cm^{-1} band, while that of Fe^{3+} completely suppressed it. These results give strong support to the aforementioned conclusion.
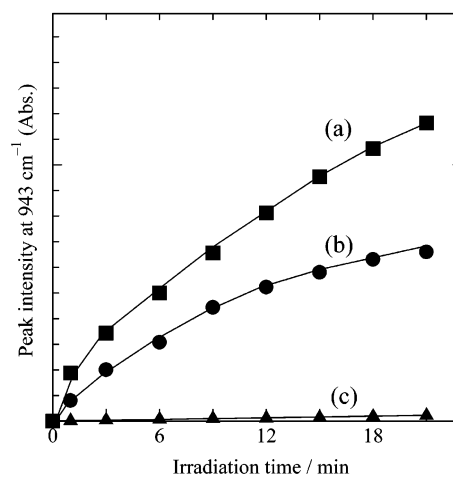

Figure 9. The band intensity at 943 cm^{-1} as a function of the UV-irradiation time in O$_2$-saturated (a) 25 wt % ethanol aqueous solution, (b) pure water, and (c) 10 mM Fe^{3+} aqueous solution.
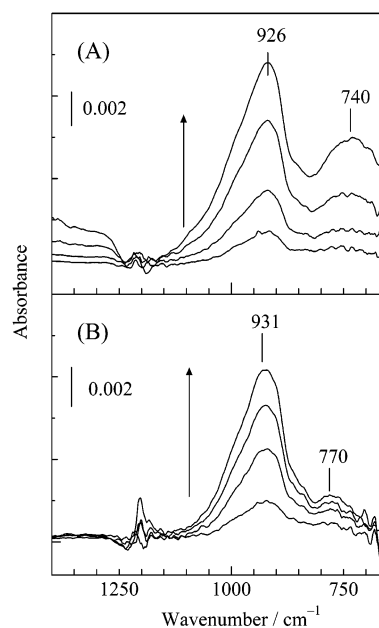

Figure 10. Time courses of MIR-IR spectra for TiO$_2$ (TIO-5) films in O$_2$-saturated D$_2$O of pD (a) 6.5 and (b) 11.2. Spectra were recorded in times of 3, 6, 12, and 24 min after the start of the UV irradiation. Arrows in the figure indicate the direction of spectral changes with time.

We also mentioned earlier that the transformation from X to Y was caused by protonation. To confirm this conclusion, we did isotope-effect experiments by using deuterated water (D$_2$O). Figure 10A and B shows the MIRIR spectra for a TiO$_2$ (TIO-5) film in O$_2$-saturated D$_2$O under neutral (pD 6.5) and alkaline (pD 11.2) conditions, respectively. Comparison of these spectra with Figure 5B and C shows that the 943 cm^{-1} (X) band in H$_2$O shifts only slightly to 926 or 931 cm^{-1} in D$_2$O. On the other hand, the 1250−1120 cm^{-1} (Y) band in H$_2$O is missing in D$_2$O, and, instead, a new band appears at about 740−770 cm^{-1} in D$_2$O. The former result for the 943 cm^{-1} band indicates that this band is inactive for H−D exchange; this band is arising from a species not containing H. On the other hand, the latter results for the 1250−1120 cm^{-1} band indicate that this band is active for the H−D exchange and arising from a protonated species, which is in harmony with the aforementioned conclusion.

We tried to investigate the chemical reactivity of species X and Y. The addition of methanol, ethanol, propanol, and carbon monoxide to the cell solution in the dark after the stop of UV illumination did not seem to change the band intensities for X and Y in a time range from 10 to 30 min, although we could not get a definite conclusion on this point because of the complex and unsteady nature of the observed spectra, probably caused by inhomogeneous slow diffusion of added reagents into the TiO_2 film. In this connection, the fact that the bands for X and Y were observed after the UV irradiation even in the presence of ethanol (Figure 8b) strongly suggests that X and Y have a low reactivity to ethanol.

We also made experiments using TiO_2 (TIO-2, anatase) films, to investigate a difference in the photoreactivity between rutile and anatase TiO_2. The experiments with TIO-2 (anatase) gave results quite similar to those of the case of TIO-5 (mainly rutile), including the pH-dependent formation of species X and Y and the transformation of X to Y in the dark, although the rate of formation of X and Y for TIO-2 is much higher than that for TIO-5 probably because of the smaller size and the larger surface area for the former. The similar behavior of rutile and anatase-type TiO_2 film gives further support to the reproducibility of the present results.

Discussion

Photocatalytic reactions on TiO_2 particles in aqueous solutions will, in general, involve various types of active intermediates, formed by reactions of both photogenerated conduction-band electrons (e^-) and valence-band holes (h^+). In the MIRIR spectra in the present work, however, intermediate species produced by photogenerated electrons (i.e., photocatalytic reduction of dissolved O_2) were observed, as mentioned in the preceding section (Figures 4 and 8). Some of photogenerated holes may be consumed to oxidize contaminating hydrocarbons at the TiO_2 surface, as indicated by the decreases in the CH-stretching band (Figure 4A). However, it is evident that the oxidation of water by photogenerated holes occurs because gas-bubble formation was clearly seen by eye in the TiO_2 film after the UV irradiation and the amount of the bubbles was increased much by the addition of Fe^{3+} to the solution. Apparently no observation of intermediates of the water oxidation might thus be attributed to either their high reactivity and short lifetime or the undesirable spectral positions of their IR bands (e.g., the O−O stretching mode of Ti−O−O−Ti as a possible intermediate[49] is reported[50,51] to be below 750 cm^{-1}).

Let us first consider the assignment of the two bands (X and Y) peaked at 943 and 1250−1120 cm^{-1}, respectively (Figure 5). Both of the bands should arise from the photocatalytic reduction of O_2, as mentioned earlier. The predominant appearance of the 943 cm^{-1} band in an alkaline solution, together with the faster appearance of the 1250−1120 cm^{-1} band in lower-pH solutions, suggests that species X is transformed to Y by protonation. That Y is a protonated species was clearly confirmed by the isotope experiment using D_2O (Figures 5 and 10). We can thus conclude, as the most plausible assignment,

that the 943 cm^{-1} band is due to a surface peroxo species, Ti-(O_2), and the 1250−1120 cm^{-1} band is due to a surface hydroperoxo species, TiOOH, respectively. The transformation of X to Y can be expressed as follows.

$$Ti(O_2) (X) + H^+ \rightarrow TiOOH (Y) \qquad (1)$$

The above assignment for species X is supported by reported IR studies of O_2 complexes of 3d metals. In general, dioxygen adducts of 3d metals show characteristic bands assigned to the O−O stretching mode in the range of 1300−600 cm^{-1}.[50−59] The bands are classified into two groups: superoxo species, MOO, exhibiting the O−O stretching band in a 1300−1100 cm^{-1} region, and peroxo species, $M(O_2)$, exhibiting the O−O stretching band in a 1000−680 cm^{-1} region.[50] For titanium adducts, it is reported that the O−O stretching band for superoxo, TiOO, lies at 1220−1140, while that for peroxo, Ti-(O_2), lies at 950−890 cm^{-1}.[51,56−59] Thus, species X having the band at 943 cm^{-1} is reasonably assigned to the peroxo species.

The assignment for species Y to surface TiOOH is derived directly from the fact that it is the first product of protonation of the surface peroxo species (eq 1). The assignment is also in harmony with reported spectral data,[60,61] although there is complexity that further protonation may proceed to some extent and resultant H_2O_2 shows bands similar to those of TiOOH. It is reported, from IR studies[60,61] of Ti-silicalite molecular sieve (TS-1) exposed to H_2O_2, that the O−O stretching band for TiOOH is at 837 cm^{-1} and that for physisorbed H_2O_2 is at 880 cm^{-1}. On the basis of the results, we can tentatively assign the bands at 838 and 887 cm^{-1} in Figure 5A to the O−O stretching modes for TiOOH and physisorbed H_2O_2, respectively. Accordingly, the 1250−1120 cm^{-1} band for Y can be assigned to the OOH bending mode for TiOOH (or TiOOH and physisorbed H_2O_2). This assignment is supported by the fact that the 838 and 887 cm^{-1} bands in Figure 5, assigned to the OO stretching for TiOOH and physisorbed H_2O_2, become stronger, with decreasing pH, in parallel with the 1250−1120 cm^{-1} band assigned to the OOH bending for the same TiOOH (and physisorbed H_2O_2). The assignment is also in harmony with an expectation that the OOH bending mode of TiOOH (1250−1120 cm^{-1}) lies at a somewhat lower energy than that of gaseous H_2O_2 (1270−1280 cm^{-1}[62−64]) because of the replacement of H by Ti.

The above assignment is further supported by the isotope experiments. Comparison of Figures 5 and 10, on the basis of the above assignment, suggests that the OO stretching band for TiOOH at 837 cm^{-1} in H_2O (Figure 5A) is shifted to a band at

(49) Kisumi, T.; Tsujiko, A.; Murakoshi, K.; Nakato, Y. *J. Electroanal. Chem.* **2003**, in press.
(50) Nakamoto, K. *Infrared and Raman Spectra of Inorganic and Coordination Compounds*; John Wiley & Sons: New York, 1986.
(51) Ohno, T.; Masaki, Y.; Hirayama, S.; Matsumura, M. *J. Catal.* **2001**, *204*, 163.
(52) Gillard, R. D.; McCleverty, J. A. *Comprehensive Coordination Chemistry*; Pergamon Press: Oxford, 1987.
(53) Andrews, L.; Chertihin, G. V.; Ricca, A.; Bauschlicher, C. W. *J. Am. Chem. Soc.* **1996**, *118*, 467.
(54) Citra, A.; Chertihin, G. V.; Andrews, L.; Neurock, M. *J. Phys. Chem. A* **1997**, *101*, 3109.
(55) Zhou, M.; Andrews, L. *J. Phys. Chem. A* **1999**, *103*, 5259.
(56) Gutsev, G. L.; Rao, B. K.; Jena, P. *J. Phys. Chem. A* **2000**, *104*, 11961.
(57) Muller, J. K.; Schwarzenbach, G. *Inorg. Chem.* **1970**, *9*, 2381.
(58) Miksztal, R.; Valentine, J. S. *Inorg. Chem.* **1984**, *23*, 3548.
(59) Kristine, F. J.; Shepherd, R. E.; Siddiqui, S. *Inorg. Chem.* **1981**, *20*, 2571.
(60) Tozzola, G.; Mantegazza, M. A.; Ranghino, G.; Petrini, G.; Bordiga, S.; Ricchiardi, G.; Lamberti, C.; Zulian, R.; Zecchina, A. *J. Catal.* **1998**, *179*, 64.
(61) Lin, W.; Frei, H. *J. Am. Chem. Soc.* **2002**, *124*, 9293.
(62) Giguere, P. A.; Srinivasan, T. K. K. *Chem. Phys. Lett.* **1975**, *33*, 479.
(63) Engdahl, A.; Nelander, B.; Karlström, G. *J. Phys. Chem. A* **2001**, *105*, 8393.
(64) Goebel, J. R.; Ault, B. S.; Del, B. J. E. *J. Phys. Chem. A* **2001**, *105*, 11365.

***Scheme 1*** . Reaction Schemes for the O₂ Reduction, Initiated by Photoexcited Electrons in the Conduction Band
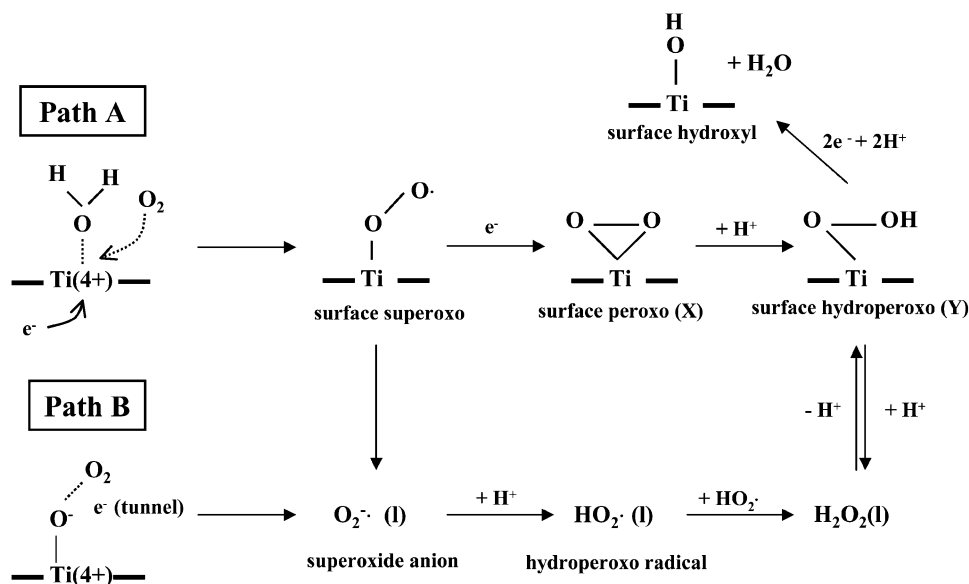
$740-770$ cm^{-1} for TiOOD in D$_2$O (Figure 10A), whereas the OOH bending band for TiOOH at $1250-1120$ cm^{-1} in H$_2$O is shifted to a band at around 900 cm^{-1} for TiOOD in D$_2$O, although the latter 900 cm^{-1} band is completely overlapping with the $926-931$ cm^{-1} band for Ti(O$_2$) and appearing only as a tail on the higher-energy side. The assignment of the $740-770$ cm^{-1} band to the OO stretching for TiOOD is supported by the fact that it becomes stronger with decreasing pH (or pD), similar to the 837 cm^{-1} band for TiOOH. Thus, the isotope shift for the OO stretching for TiOOH is calculated to be $97-67$ cm^{-1}, and that for the OOH bending is $350-220$ cm^{-1}. These values are quite reasonable, as compared to the reported shifts for gaseous H$_2$O$_2$ by monodeuteration from H$_2$O$_2$ to HDO$_2$, about 80 cm^{-1} for the O−O stretching mode and 290 cm^{-1} for the OOH bending mode.[63,65]

On the basis of the above assignment for species X and Y, we can propose a possible reaction scheme for the photocatalytic reduction of O$_2$ at the TiO$_2$ surface, as shown in Scheme 1. The reduction of O$_2$ may be initiated by electron capture at H$_2$O-adsorbed Ti(4+) sites, immediately followed by an attack of an O$_2$ molecule, leading to the formation of the superoxo species, TiOO•, as a precursor of the surface peroxo species, Ti(O)$_2$, although TiOO• was not detected in the present work probably because of its short lifetime. It is well established in a vacuum or gaseous systems that photogenerated electrons are captured at surface Ti(4+) sites to produce Ti(3+) sites, using low-temperature ESR measurements under controlled atmospheres[13,14,66] as well as surface analyses with XPS, SHG, and TPD.[67−70] O$_2$ can readily attack them, resulting in, for example, the superoxo species. The surface peroxo species, Ti(O$_2$), is formed by further reduction of TiOO• with an electron. Ti(O$_2$)

has a closed-shell electronic structure and is expected to be fairly stable.

It is to be noted that Scheme 1 is in harmony with other features of the observed spectral changes. A significant decrease in the band intensity for the OH stretching mode of water at 3377 cm^{-1} (spectrum c of Figure 4A) can be explained by a decrease in the amount of water within the TiO$_2$ film, caused by accumulation of tiny O$_2$ (or CO$_2$) gas bubbles produced by oxidative reactions of photogenerated holes. The explanation is supported by the enhancement of the decrease in the intensity of the OH stretching band by addition of Fe^{3+} ions to the solution.

The 1023 cm^{-1} band appearing in a neutral solution (Figure 5B), which is weak in an acidic solution (Figure 5A) and nearly absent in an alkaline solution (Figure 5C), is active for the isotopic H−D exchange (compare Figures 5B and 10), indicating that the corresponding species contains H atoms. A tentative assignment of this band is the O−O stretching mode of the hydroperoxo radicals, HO$_2$•, present in the solution phase (Scheme 1). Recent negative-ion photoelectron spectroscopy showed that the hydroperoxo radicals had the O−O stretching mode at 1102 cm^{-1} at 200 K.[71] The pK_a of HO$_2$• is 4.88, and thus it is transformed into O$_2^-$• radicals in alkaline solutions, which can explain the absence of the 1023 cm^{-1} band in an alkaline solution. On the other hand, in acidic solutions, an effective disproportionation reaction may occur with H$^+$ ions as a catalyst

$$HO_2• + HO_2• \rightarrow H_2O_2 + O_2 \qquad (2)$$
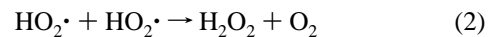
which leads to a decrease in the HO$_2$• concentration. The HO$_2$• radicals in solution can be produced either via desorption of surface superoxo radicals, TiOO•, or via direct electron transfer from the TiO$_2$ conduction band to adsorbed O$_2$, both followed by protonation. The latter direct electron transfer can be effective in alkaline solutions, as observed at single-crystal TiO$_2$ (rutile) electrodes.[72]

(65) Pettersson, M.; Tuominen, S.; Räsänen, M. *J. Phys. Chem. A* **1997**, *101*, 1166.
(66) Anpo, M.; Kubokawa, Y.; Fujii, T.; Suzuki, S. *J. Phys. Chem.* **1984**, *88*, 2512.
(67) Shultz, A. N.; Jang, W.; Hetherington, W. M.; Baer, D. R.; Wang, L.-Q.; Engelhard, M. H. *Surf. Sci.* **1995**, *399*, 114.
(68) Shultz, A. N.; Hetherington, W. M.; Baer, D. R.; Engelhard, M. H.; Wang, L.-Q. *Surf. Sci.* **1997**, *392*, 1.
(69) Henderson, M. A.; Epling, W. S.; Perkins, C. L.; Peden, C. H. F.; Diebold, U. *J. Phys. Chem. B* **1999**, *103*, 5328.
(70) Linsebigler, A.; Lu, G.; Yates, J. T., Jr. *J. Phys. Chem.* **1996**, *100*, 6631.

(71) Ramond, T. M.; Blanksby, S. J.; Kato, S.; Bierbaum, V. M.; Davico, G. E.; Schwartz R. L.; Lineberger, W. C.; Ellison, G. B. *J. Phys. Chem. A* **2002**, *106*, 9641.

It is finally to be noted that the observed spectral changes (Figures 4−10), especially the band intensities, are more or less affected by reactions of the (electron-induced) intermediates in Scheme 1 with photogenerated holes or hole-induced intermediates (a kind of reverse reaction). Further detailed studies are necessary to get definite conclusions on these reactions. Such studies are now underway.

Conclusions

The MIRIR technique has allowed the in situ direct detection of surface intermediates of the photocatalytic O_2 reduction at the TiO_2 surface in aqueous solutions, proving that it is really a powerful tool for mechanistic studies. Detailed investigations under various conditions have revealed that the surface peroxo species, $Ti(O_2)$, is primarily produced, probably via $Ti-OO\cdot$ as a precursor, which is then transformed to the surface hydroperoxo, TiOOH, by protonation in the dark. The present work has also revealed that the rates of the primary steps strongly depend on the pH solution, thus opening a new possibility of control of successive reaction processes by a change of the solution pH. Further studies of the primary mechanisms of photocatalytic reactions will serve as a control or for improvement of complex photocatalytic reactions in various application fields.

JA029503Q

(72) Tsujiko, A.; Itoh, H.; Kisumi, T.; Shiga, A.; Murakoshi, K.; Nakato, Y. *J. Phys. Chem. B* **2002**, *106*, 5878.